Spatial Coordination of Electromagnetic Communication Infrastructure, AI Technology Attention and Regional E-commerce Development: Evidence from China

Kai Pei[1], Zhongxuan Fu[2*], Shutong Meng[3], Wang Jing[4]
[1]School of Accountancy, Shandong University of Finance and Economics, Shandong, China
[2]Ally Bridge Group (HK) Limited, HongKong, China
[3]Crowe LLP, Limited Liability Partnership, USA
[4]School of Business, Shandong Jianzhu University, Shandong, China

Corresponding author: Zhongxuan Fu (e-mail: elinafu0125@gmail.com).

ABSTRACT The digital economy rests on a physical substrate that is entirely electromagnetic: every transaction it records travels either as a guided optical wave in the fiber transport network or as a free-space radio wave across the mobile access link. These two layers obey different physics and therefore different deployment economics, yet regional studies of digital-economy development collapse them into a single infrastructure variable. This paper builds a three-system coupling coordination framework linking electromagnetic communication infrastructure, public attention to artificial intelligence (AI), and regional ecommerce development across 31 Chinese provinces from 2012 to 2022. The infrastructure system is resolved into a guided-wave layer, measured by long-haul optical cable route length, route density per square kilometer and broadband access ports, and a free-space layer, measured by mobile switching capacity, its areal density and mobile telephone penetration, because path-loss-limited areal coverage and length-proportional transport scale differently with provincial geography. Subsystem levels are obtained by entropy-weighted TOPSIS and combined through a coupling coordination model generalized to $n = 3$. A binding-constraint diagnostic then identifies, for each province and year, whether the electromagnetic layer rather than demand limits coordination, and whether the constraint originates in transport or in access. Coordination rises from 0.293 to 0.448 and is spatially clustered in every year, with Moran's I falling from 0.418 to 0.296 while remaining significant at the 1% level; relative dispersion narrows, and inter-regional differences supply about 71% of what remains. The binding subsystem migrates from demand to physical capacity: the electromagnetic layer binds in no province in 2012 but in 14 of 31 by 2022, and 82% of constrained observations are access-limited, concentrated in provinces that are systematically larger in area and more thinly settled.

INDEX TERMS optical fiber networks, radio access networks, network deployment density, wave propagation and coverage, digital infrastructure, coupling coordination degree

I. INTRODUCTION

THE digital economy is usually described in the language of platforms, algorithms and business models, but every transaction it records is ultimately a physical event in an electromagnetic channel. A product query, a recommendation request, a payment confirmation and a logistics update all propagate as guided optical waves along the fiber transport network and as free-space radio waves over the final hundreds of meters to the user terminal. The throughput, latency and geographical reach of commerce are therefore bounded, in the last instance, by the electromagnetic infrastructure that has actually been deployed. That bound is not uniform in space. Guided-wave transport is a length-proportional asset: its capacity is set by the spectral efficiency attainable in the fiber [1], [2], while its cost is dominated by civil works and therefore scales with route kilometers. Free-space access is an area-coverage asset: its cost scales with the number of radio sites needed to overcome path loss across a service area, and its attainable rate degrades with link distance and with the carrier frequency selected [3], [4]. Two provinces with identical economic aggregates but different land areas and settlement densities thus face structurally different costs of delivering the same electromagnetic service level.

China offers an unusually informative setting in which to examine this asymmetry, because between 2012 and 2022 three processes unfolded simultaneously and at scale. First, public and industrial attention to artificial intelligence rose sharply. The AI Index 2024 report released by Stanford University notes that China and the United States dominate the global AI race. Between 2021 and 2022 global AI patent grants rose by 62.7%, of which China secured 61.1% against the United States' 20.9%. Over 2013–2022 China's share of global industrial robot installations grew from 20.8% to 52.4%, reaching 290,300 installations in the final year. Second, China became the world's largest e-commerce market, with AI moving from search-ranking and payment security into personalized recommendation, conversational customer service and, more recently, generative retrieval. Third, and least studied, China carried out one of the largest programs of optical-fiber and mobile base-station construction ever undertaken, extending long-haul fiber routes, converting copper access to fiber-to-the-premises, and densifying radio sites, overwhelmingly in the sub-6 GHz bands, where China concentrated its fourth- and fifth-generation deployment; millimeter-wave spectrum remained at the trial stage throughout the sample period. All three processes were highly uneven across provinces, and there is no reason to expect them to have advanced in step.

Existing regional research nevertheless treats the electromagnetic layer either as a control variable or as one dimension nested inside a composite digital-economy index. Two consequences follow. First, the guided-wave and free-space layers are aggregated, so precisely the asymmetry that propagation physics predicts is averaged away: a province rich in transit fiber but sparse in radio sites is scored identically to its mirror image. Second, because infrastructure is nested inside the outcome index, one cannot ask the question that matters for deployment planning, namely whether the physical layer is the factor actually limiting realized commercial activity. A related measurement problem has gone largely unremarked: when broadband subscriber counts enter the outcome index while search-volume data proxy demand, the two constructs share the internet-user base as a common driver, and part of their measured association is mechanical rather than economic.

This paper addresses both problems by promoting electromagnetic infrastructure from a control to a co-equal subsystem, and by resolving it into the two layers that the underlying physics distinguishes. We ask three questions.

(Q1) How has coordination among the electromagnetic layer, AI technology attention and e-commerce development evolved across Chinese provinces, and how is it distributed in space?

(Q2) Where and when is the electromagnetic layer the binding constraint, and does that constraint originate in guided-wave transport or in radio access?

(Q3) What accounts for the observed spatial and distributional pattern?

A coupling coordination framework rather than a single-equation regression is appropriate to these questions because the object of interest is not the marginal effect of one variable upon another, but the degree to which three subsystems that must advance together actually do so. A regression coefficient cannot express the state of a province that is simultaneously high in demand and low in physical capacity, whereas a coordination measure is defined precisely on that mismatch.

The contributions are fourfold. First, we construct what is, to our knowledge, the first provincial indicator system for China's electromagnetic communication infrastructure that separates the guided-wave and free-space layers and expresses each in areal-density as well as absolute terms, so that coverage economics rather than economic scale drives the measurement. Second, we generalize the coupling coordination model from $n = 2$ to $n = 3$ and show that the conventional two-system expression is its special case, allowing demand and physical capacity to be assessed jointly rather than sequentially. Third, we introduce a binding-constraint diagnostic that converts the coordination measure into an actionable statement about which layer to build next, and we distinguish fiber-limited from access-limited provinces. Fourth, we remove the mechanical component of the attention-development association by excluding subscriber counts from the outcome index and by normalizing search volume by resident population rather than by the internet-user base, which would otherwise tie demand back to the infrastructure subsystem. The remainder of the paper is organized as follows. Section II sets out the physical and deployment characteristics of the two electromagnetic layers and derives three testable hypotheses. Section III reviews the related literature. Section IV describes the data, the indicator systems and the methods. Section V reports the results. Section VI discusses their implications and limitations, and Section VII concludes.

II. THE ELECTROMAGNETIC LAYER: PROPAGATION PHYSICS AND DEPLOYMENT ECONOMICS

A. GUIDED-WAVE TRANSPORT

The transport tier of any commercial data network is a low-loss dielectric waveguide. Single-mode silica fiber operated in the 1550 nm window exhibits attenuation of approximately 0.2 dB/km, which permits amplified spans of the order of 80–100 km and transcontinental reach with optical amplification alone [5]. Capacity on an installed route is raised not by adding route length but by adding wavelengths and by increasing the spectral efficiency of each carrier through higher-order modulation and coherent detection. Both levers are bounded: the nonlinear Shannon limit places a ceiling on the information spectral density achievable in a given fiber, and the industry response has been successive additions of parallelism, in wavelength, in polarization and, prospectively, in space [1], [2], [6].

Two features of this technology matter for regional analysis. The first is that the cost of guided-wave transport is dominated by civil works and scales with route kilometers, essentially independently of the area or the population served. The second is that a long-haul route traversing a province may serve traffic that neither originates nor terminates there, so absolute route length partly reflects transit geography rather than local provisioning. For this reason we characterize the guided-wave layer by route length and by route density per unit area jointly, and we add broadband access ports, which measure how far the guided-wave medium has been extended toward the end user rather than merely between cities. Fiber-to-the-premises penetration would serve the same purpose but is not published as a provincial series for the sample period.

B. FREE-SPACE RADIO ACCESS

The access tier obeys quite different physics. For a transmitter of given effective isotropic radiated power and a receiver of given sensitivity, received power falls approximately as d^{-v}, where the path-loss exponent v is near 2 in free space and typically between 3 and 4 in built environments. The Friis relation adds a second penalty: for fixed antenna gains, loss rises with carrier frequency, because the effective aperture shrinks with the square of the wavelength [3]. Millimeter-wave carriers add atmospheric absorption, rain attenuation, foliage loss and severe sensitivity to blockage [7]. Consequently the cell radius sustainable at a given link budget contracts as the carrier frequency rises, and the number of sites required to cover a service area of extent A grows roughly in proportion to A divided by the square of that radius.

This produces the coverage-capacity trade-off that has organized a decade of radio engineering: sub-6 GHz spectrum provides reach with limited bandwidth, while millimeter-wave spectrum provides bandwidth over very short ranges [4], [7]. The engineering response has been to raise the capability of the individual site and terminal rather than simply to multiply sites, through multiple-input multiple-output arrays and beamforming, through wideband and multiband radiators, and through miniaturized high-gain elements that can be integrated into compact terminals. Recent work in this journal is representative of that program: compact four-port MIMO geometries for the 28 and 38 GHz millimeter-wave bands [8], miniaturized fractal radiators for the 6 GHz band [9], super-wideband graphene-based monopoles [10], and planar high-gain circularly polarized elements for the 2.45 GHz ISM band [11]. Each such advance shifts the deployment frontier by lowering the number of sites, or the site cost, required to deliver a target service level over a given area.

The regional implication is direct. Because coverage is an areal problem, the propagation-relevant measure of radio infrastructure is site density per unit area, not site count. A province of large extent and low settlement density must fund far more sites per subscriber to reach the same coverage probability than a compact, densely settled one, and this penalty is imposed by propagation rather than by economic backwardness. It is therefore a testable proposition, rather than an assumption, that the free-space layer binds earlier than the guided-wave layer in China's western provinces.

C. WHY AI-INTENSIVE COMMERCE RAISES THE ELECTROMAGNETIC THRESHOLD

Catalogue e-commerce of the kind that prevailed early in the sample period was tolerant of the physical layer. Its payload was text and compressed still images, its traffic was strongly downlink-dominated, and interaction latencies of several hundred milliseconds were acceptable. AI-mediated commerce relaxes none of these conditions. Real-time personalized recommendation requires an inference result to be returned inside an interactive latency budget; conversational customer service imposes continuous low-latency bidirectional exchange; visual and voice search, and above all livestream selling, impose sustained uplink demand, which is the scarcer direction in the time-division duplex configurations used across most of China's mobile spectrum. Where inference is pushed to the network edge to meet those budgets, the placement of compute becomes coupled to the topology of the radio access network itself [12]. The service classes anticipated for sixth-generation systems extend this dependence further, since their latency and reliability targets are stated in terms that only a dense and compute-adjacent access network can meet [13].

It follows that attention to AI does not convert into realized e-commerce activity at a fixed rate. The conversion is conditional on the electromagnetic layer, and the elasticity of that conversion should be lower where the layer is thin. This is the substantive reason for treating infrastructure as a third subsystem rather than as a regressor: the object to be measured is a three-way correspondence between what a region wants, what it can physically carry, and what it actually transacts.

D. HYPOTHESES

H1. The coordination degree among the three subsystems exhibits positive spatial autocorrelation. Both fiber routes and radio coverage are contiguous network assets whose value at any point depends on connectivity to adjacent points, so deployment should spill across provincial borders rather than stop at them.

H2. In provinces of large land area and low settlement density, the free-space layer binds more frequently than the guided-wave layer, because coverage cost scales with area whereas transport cost scales with route length.

H3. The shortfall of realized e-commerce development relative to AI technology attention is larger where the electromagnetic layer is the binding subsystem, and narrows as that constraint is relieved.

III. LITERATURE REVIEW

A. CAPACITY AND DEPLOYMENT OF ELECTROMAGNETIC COMMUNICATION INFRASTRUCTURE

The engineering literature on communication infrastructure is largely concerned with capacity per unit of deployed asset. On the guided-wave side, Essiambre and Tkach set out the capacity trends and fundamental limits of optical transport and identified the nonlinear ceiling that has since organized research on spatial-division multiplexing [1], while Winzer, Neilson and Chraplyvy reviewed two decades of fiber-optic transmission and networking and argued that further growth must come from parallelism rather than from spectral efficiency alone [2]. On the free-space side, Rappaport and colleagues established the measurement basis for millimeter-wave mobile access and showed that the band is usable despite its propagation penalties [7], and Andrews and colleagues set out the densification and coverage-capacity trade-offs that follow [4]. Mao and colleagues surveyed mobile edge computing and made explicit the dependence of latency-bounded services on radio-access topology [12]. Within this journal, work on compact millimeter-wave MIMO arrays [8], miniaturized 6 GHz radiators [9], super-wideband monopoles [10] and high-gain ISM-band elements [11] has progressively reduced the site and terminal cost of a given coverage target.

What this literature does not address, because it is not its purpose, is the spatial economics of deployment at the scale of a national administrative geography: which regions in fact possess how much of each layer, whether the two layers advance together, and which layer limits the services built on top of them. That question requires provincial panel measurement rather than link-level or device-level analysis, and it is the gap this paper addresses.

B. MEASURING TECHNOLOGY ATTENTION

Search-engine query volume has become a standard proxy for public attention because it is revealed rather than stated, is available at fine temporal and spatial resolution, and precedes rather than follows adoption. In the Chinese context the Baidu Index plays the role that Google Trends plays elsewhere. Two cautions are well established and are adopted here. Query volume scales with the size of the searching population, so raw provincial indices are not comparable across provinces and must be scaled by a measure of that population before any cross-sectional statement is made; Section IV explains why resident population rather than the internet-user base is the appropriate denominator here. And attention is not capability: a high index records interest, expectation or concern, not deployed technical capacity. Where AI is concerned, Davenport and colleagues document the specific commercial functions through which the technology enters marketing and customer interaction [14], which is the channel by which attention plausibly becomes traffic.

C. E-COMMERCE DEVELOPMENT AND ITS INFRASTRUCTURAL DETERMINANTS

Research on e-commerce development has consistently identified frictions that are logistical, institutional or informational rather than physical-layer. Gomez-Herrera, Martens and Turlea show that language barriers together with logistics and payment costs constrain cross-border digital trade in the European Union [15]. Kim and Peterson, in a meta-analysis of online trust relationships, establish trust as a central mediator between platform characteristics and transaction outcomes [16]. Ma, Chai and Zhang characterize cross-border e-commerce in China as a distinct trade channel combining goods trade with digital technology [17]. Hovelaque, Soler and Hafsa model the supply-chain consequences of e-commerce order fulfilment, comparing store-picking, warehouse-picking and drop-shipping configurations [18], and Andonov, Dimitrov and Totev report the firm-level performance effects of e-commerce adoption [19].

This body of work treats connectivity as a background condition. That was a reasonable simplification when the marginal service was a catalogue page, but it is no longer reasonable when the marginal service is an inference request with an interactive latency budget and a sustained uplink requirement. The present paper therefore brings the physical layer into the foreground and asks whether it, rather than trust, logistics or demand, is the operative constraint in a given region and year.

In summary, the engineering literature measures the capability of the electromagnetic layer without locating it in economic geography; the attention literature measures demand without reference to the medium that must carry it; and the e-commerce literature measures outcomes while holding connectivity implicit. No existing study, to our knowledge, measures all three at provincial resolution, separates the guided-wave and free-space layers according to their distinct deployment economics, and asks which of the three is binding. That is the contribution attempted here.

IV. RESEARCH DESIGN

Two clarifications govern the interpretation of everything that follows. First, this study measures public attention to AI technologies, not the development or deployment of AI systems themselves. The Baidu Index records query volume for AI-related terms, which proxies awareness, interest and expectation. Accordingly the coordination degree computed below expresses the correspondence among attention, physical carrying capacity and realized commercial activity; it is not a measure of technical coupling between AI systems and network equipment. Second, because query volume scales with the size of the searching population, every keyword series is divided by the provincial resident population before entering the index, so that the resulting measure is search intensity rather than search volume and is comparable across provinces. Population rather than the internet-user base is used as the denominator deliberately: broadband subscribers now belong to the infrastructure subsystem, and normalizing demand by them would reintroduce between U1 and U2 exactly the mechanical association that relocating them was intended to remove.

On the temporal validity of the keyword set, the term AGI became prominent as an independent search term only after 2022. The index is therefore built on a multi-dimensional keyword system whose remaining terms—machine learning, deep learning, natural language processing, speech recognition and the application-scenario terms listed in Table I—have been actively searched in China since 2012. As a robustness check the entire analysis is repeated with AGI excluded; excluding AGI leaves the subsystem index correlated with the baseline at above 0.99 and changes none of the conclusions reported below.

A. SAMPLE AND DATA

The sample comprises the 31 provinces, autonomous regions and municipalities of mainland China over 2012–2022, giving 341 province-year observations. Three subsystems are measured.

U1, AI technology attention, is built from Baidu Index series for fourteen keywords grouped into core concepts and technologies, data processing and analysis, and application scenarios, each normalized by provincial resident population as described above. The indicator definitions are given in Table I, Panel A.

Six terms represent core concepts and technologies. Artificial general intelligence denotes a system able to perform any intellectual task at or beyond the human level, so its search volume tracks interest in the frontier of the field. Autonomous learning captures attention to adaptive and self-optimizing methods. Machine learning is the central paradigm of contemporary AI and provides the broadest single measure of technical interest. Deep learning, dominant in image recognition, indexes attention to the methods behind recent performance gains. Natural language processing underpins machine translation and conversational interfaces, and therefore tracks interest in human-machine communication. Speech recognition, embedded in smart-home and voice-assistant products, records attention to the voice modality specifically.

Three terms represent data processing and analysis. Data visualization concerns the graphical presentation of data and indexes interest in data-driven decision support. Data mining concerns the extraction of patterns from large datasets and indexes interest in analytical capability. Business intelligence spans the collection, management and analysis of enterprise data, and indexes interest in decision-support systems inside firms.

Five terms represent application scenarios. Intelligent customer service, built on natural language processing and machine learning, indexes interest in automating service interactions. Personalized recommendation, which infers preferences from behavioral data, indexes interest in optimizing the user experience. Human-computer interaction indexes interest in interface design. Intelligent marketing, which applies analytics to targeting and campaign design, indexes interest in data-driven commercial practice. Biometrics, used in authentication and payment verification, indexes interest in identity and security technologies.

U3, regional e-commerce development, is built from enterprise informatization and e-commerce activity indicators drawn from the China Statistical Yearbook. It differs from the specification used in earlier work on this topic in one important respect: the two digital-infrastructure indicators previously included here, long-haul fiber length and broadband subscribers, have been removed and relocated to the infrastructure subsystem. This eliminates the double counting of physical capacity and removes the mechanical correlation between U1 and U3 that a shared internet-user base would otherwise induce. The indicator definitions are given in Table I, Panel B.

Enterprise informatization is measured by three indicators. The share of enterprises using computers captures the basic diffusion of information technology. The share with a website captures the capacity to present and market products online. The share adopting information-technology management captures how far firms have digitized internal coordination and decision-making.

E-commerce activity is measured by five indicators. The share of enterprises engaged in e-commerce transactions measures market participation. The share with e-commerce sales measures the extent of online selling, and the share with e-commerce procurement measures the use of digital channels on the input side; the latter carries the largest entropy weight in this panel. Total e-commerce sales measure the scale of the market and its direct economic contribution, while total e-commerce purchases measure the depth of digital procurement in the supply chains of firms.

U2, electromagnetic communication infrastructure, is the subsystem introduced in this paper and is resolved into the two layers distinguished in Section II. The guided-wave layer comprises long-haul optical cable route length, optical cable route density per square kilometer, and internet broadband access ports. The free-space layer comprises mobile switching capacity, mobile switching capacity density per square kilometer, and mobile telephone penetration per hundred persons. Density measures enter alongside absolute measures precisely because, as Section II argues, coverage is an areal problem while transport is a length problem; the entropy procedure in fact assigns the largest single weight in the subsystem, 0.436, to switching capacity density. One measurement choice requires comment. Provincial counts of radio base stations are not published in the Chinese statistical system for the sample period, so the free-space layer is measured by mobile switching capacity, which is the deployment-capacity variable used for this purpose throughout the provincial digital-economy literature. It is a proxy for installed network capacity rather than a count of radio sites, and Section VI returns to what that substitution can and cannot support. Communications indicators are taken from the China Statistical Yearbook and the annual communications-industry statistics compiled from it; provincial land areas, used to form the density measures, and resident population are taken from the same source. The indicator definitions and entropy weights are given in Table I, Panel C.

Two further data limitations are stated explicitly. Provincial 5G site counts are published only from 2019 and provincial radio-site counts not at all, so neither can enter an index spanning 2012–2022; this is the reason for the switching-capacity proxy described above. And provincial mobile internet data traffic is available only from 2014, so it is excluded from the index and used only as a robustness check.

B. RESEARCH METHODOLOGY

1) TOPSIS-Entropy Method

This study employs the entropy-weighted TOPSIS method [20], with indicator weights derived from the Shannon information entropy of each series [21], to assess AI technology attention, electromagnetic infrastructure and e-commerce development. The steps are as follows:

Let X be the $n \times m$ raw indicator matrix, where n is the number of objects (province-years) and m the number of indicators.

$$X = \begin{bmatrix} x_{11} & x_{12} & \cdots & x_{1m} \\ x_{21} & x_{22} & \cdots & x_{2m} \\ \vdots & \vdots & \ddots & \vdots \\ x_{n1} & x_{n2} & \cdots & x_{nm} \end{bmatrix} \tag{1}$$

The raw matrices were normalized using the polar deviation method.

Positive indicators:

$$z'_{ij} = \frac{x_{ij} - x_j^{\min}}{x_j^{\max} - x_j^{\min}} \tag{2}$$

Negative indicators:

$$z'_{ij} = \frac{x_j^{\max} - x_{ij}}{x_j^{\max} - x_j^{\min}} \tag{3}$$

The value of object i on indicator j is then expressed as a share of that indicator's column total, P_{ij}, giving the normalized matrix Z:

$$Z = \begin{bmatrix} z_{11} & z_{12} & \cdots & z_{1m} \\ z_{21} & z_{22} & \cdots & z_{2m} \\ \vdots & \vdots & \ddots & \vdots \\ z_{n1} & z_{n2} & \cdots & z_{nm} \end{bmatrix} \tag{4}$$

where

$$P_{ij} = \frac{z_{ij}}{\sum_{i=1}^{n} z_{ij}}, \qquad (j = 1, 2, \ldots, m) \tag{5}$$

Compute the information entropy E_j of indicator j.

$$E_j = -\frac{1}{\ln n} \sum_{i=1}^{n} P_{ij} \ln P_{ij}, \qquad (j = 1, 2, \ldots, m) \tag{6}$$

Compute the coefficient of variation G_j of indicator j.

$$G_j = 1 - E_j \tag{7}$$

Compute the weight W_j of indicator j.

$$W_j = \frac{G_j}{\sum_{j=1}^{m} G_j} \tag{8}$$

Construct the weighted matrix by multiplying each column of Z by its corresponding weight.

$$Z = \begin{bmatrix} \omega_1 * z_{11} & \omega_2 * z_{12} & \cdots & \omega_m * z_{1m} \\ \omega_1 * z_{21} & \omega_2 * z_{22} & \cdots & \omega_m * z_{2m} \\ \vdots & \vdots & \ddots & \vdots \\ \omega_1 * z_{n1} & \omega_2 * z_{n2} & \cdots & \omega_m * z_{nm} \end{bmatrix} \tag{9}$$

The weighted matrix is:

$$Z = \begin{bmatrix} z_{11} & z_{12} & \cdots & z_{1m} \\ z_{21} & z_{22} & \cdots & z_{2m} \\ \vdots & \vdots & \ddots & \vdots \\ z_{n1} & z_{n2} & \cdots & z_{nm} \end{bmatrix} \tag{10}$$

Positive Ideal Solution:

$$Z^+ = (Z_1^+, Z_2^+, \ldots, Z_m^+) \tag{11}$$

Negative Ideal Solution:

$$Z^- = (Z_1^-, Z_2^-, \ldots, Z_m^-) \tag{12}$$

Use Euclidean distances to calculate the distance of an object from positive and negative ideal solutions.

$$D_i^+ = \sqrt{\sum_{j=1}^{m} (Z_j^+ - z_{ij})^2} \tag{13}$$

$$D_i^- = \sqrt{\sum_{j=1}^{m} (Z_j^- - z_{ij})^2} \tag{14}$$

Relative closeness was calculated and ranked using negative ideal solution distances.

$$S_i = \frac{D_i^-}{D_i^+ + D_i^-} \tag{15}$$

Coupling coordination evaluation model

Because this study evaluates three subsystems rather than two, the coupling degree is computed from the n-system form of the model,

$$C = n \sqrt[n]{\frac{U_1 \times U_2 \times \cdots \times U_n}{(U_1 + U_2 + \cdots + U_n)^n}} \tag{16}$$

of which the two-system expression used in earlier applications is the special case $n = 2$. Setting $n = 3$ and writing U1, U2 and U3 for AI technology attention, electromagnetic infrastructure and e-commerce development

TABLE 1. Indicator Evaluation System: Panel A AI Technology Attention, Panel B Regional E-Commerce Development, Panel C Electromagnetic Communication Infrastructure

Dimension	Norm	Entropy	Coefficient of variation	Weights	Arrange in order
Panel A: AI technology attention (U1)					
Application scenario	Intelligent Marketing	0.789	0.211	0.159	1
Application scenario	Intelligent Customer Service	0.800	0.200	0.151	2
Application scenario	Personalized Recommendation	0.879	0.121	0.091	3
Core concepts	Natural Language Processing	0.884	0.116	0.088	4
Application scenario	Biometrics	0.908	0.092	0.069	5
Core concepts	Deep Learning	0.915	0.085	0.064	6
Data processing	Data Visualization	0.915	0.085	0.064	7
Data processing	Business Intelligence	0.916	0.084	0.064	8
Core concepts	AGI	0.921	0.079	0.059	9
Core concepts	Machine Learning	0.937	0.063	0.048	10
Application scenario	Human-computer Interaction	0.945	0.055	0.042	11
Core concepts	Speech Recognition	0.949	0.051	0.039	12
Data processing	Data Mining	0.952	0.048	0.036	13
Core concepts	Autonomous Learning	0.966	0.034	0.026	14
Panel B: regional e-commerce development (U3)					
E-commerce activity	Share of enterprises with e-commerce procurement	0.960	0.040	0.326	1
E-commerce activity	Share of enterprises with e-commerce sales	0.973	0.027	0.216	2
E-commerce activity	Share of enterprises with e-commerce transactions	0.976	0.024	0.192	3
Enterprise informatization	Share of enterprises with a website	0.989	0.011	0.090	4
E-commerce activity	E-commerce sales	0.992	0.008	0.065	5
E-commerce activity	E-commerce purchases	0.994	0.006	0.051	6
Enterprise informatization	Share of enterprises adopting IT management	0.995	0.005	0.037	7
Enterprise informatization	Share of enterprises using computers	0.997	0.003	0.024	8
Panel C: electromagnetic communication infrastructure (U2)					
Free-space layer	Mobile switching capacity density (per km^2)	0.850	0.150	0.436	1
Guided-wave layer	Internet broadband access ports	0.947	0.053	0.155	2
Guided-wave layer	Optical cable route density (km per km^2)	0.954	0.046	0.134	3
Free-space layer	Mobile switching capacity	0.961	0.039	0.115	4
Guided-wave layer	Long-haul optical cable route length	0.967	0.033	0.095	5
Free-space layer	Mobile telephone penetration (per 100 persons)	0.978	0.022	0.064	6

respectively gives the coupling degree used throughout this paper. The comprehensive coordination index becomes

$$T = \alpha U_1 + \beta U_2 + \gamma U_3 \tag{17}$$

with alpha = beta = gamma = 1/3, so that no subsystem is privileged a priori, and the coupling coordination degree D is obtained from C and T exactly as in the two-system case. The classification thresholds of Table II are retained.

The coupling coordination degree D is then obtained as

$$D = \sqrt{C \times T} \tag{18}$$

The computed coupling coordination degree D is matched to the corresponding interval to obtain its coordination level (see Table II).

C. BINDING-CONSTRAINT DIAGNOSTIC

The coupling coordination degree D summarizes how evenly the three subsystems have advanced, but it does not say which of them is furthest behind. Since that is precisely the question a deployment planner asks, we define a binding-constraint diagnostic. For province i in year t, let the binding subsystem be the one attaining the lowest normalized level,

$$k^*(i,t) = \arg\min_k U_k(i,t), \qquad k \in \{1,2,3\} \tag{19}$$

and let the severity of the constraint be the shortfall of that subsystem below the mean of the three,

$$\lambda(i,t) = \frac{\overline{U}(i,t) - U_{k^*}(i,t)}{\overline{U}(i,t)} \tag{20}$$

where the bar denotes the mean of the three subsystem levels, so that lambda equals zero when the three subsystems are perfectly balanced and rises as one falls behind. A province-year is classified as electromagnetically constrained when the binding subsystem is U2. For such observations the constraint is attributed to a layer by comparing the guided-wave and free-space sub-indices,

$$\delta(i,t) = U_2^G(i,t) - U_2^F(i,t) \tag{21}$$

where a positive value indicates that radio access lags guided-wave transport, so that the province is access-limited, and a negative value indicates the converse, fiber-limited, case. Hypothesis H2 predicts that access-limited observations will be concentrated in provinces of large area and low settlement density.

D. DISTRIBUTIONAL AND SPATIAL METHODS

1) Kernel Density Estimation

We apply kernel density estimation [22] to investigate the time-evolution dynamics of the three subsystems and of their

TABLE 2. Table of Coupling Coordination Types

Starting value (closed)	End value (on)	Level of coordination
0	0.1	1
0.1	0.2	2
0.2	0.3	3
0.3	0.4	4
0.4	0.5	5
0.5	0.6	6
0.6	0.7	7
0.7	0.8	8
0.8	0.9	9
0.9	1	10

coupling coordination degree. The calculation formula is shown below:

$$f(x) = \frac{1}{Nh}\sum_{i=1}^{n} K\left(\frac{X_i - x}{h}\right) \tag{22}$$

$$K = \frac{1}{\sqrt{2\pi}} \exp\left(-\frac{x^2}{2}\right) \tag{23}$$

where x is the point at which the density is evaluated, N is the number of observations, h is the bandwidth, K is the Gaussian kernel function and X_i are the independent identically distributed observations. Bandwidth is selected by Silverman's rule of thumb, and the estimates are verified to be insensitive to that choice.

2) Spatial Autocorrelation Analysis

Global and local spatial correlation of the coupling coordination degree is measured with Moran's I statistic [23] and its local decomposition [24]. The calculation formula is shown below:

$$\text{Moran's } I = \frac{n\sum_{i=1}^{n}\sum_{j=1}^{n} W_{ij}(x_i - \overline{X})(x_j - \overline{X})}{\sum_{i=1}^{n}\sum_{j=1}^{n} W_{ij} \sum_{i=1}^{n}(x_i - \overline{X})^2} \tag{24}$$

where W_{ij} is the spatial weight matrix and n the number of spatial units. Decomposing Moran's I over individual units gives the local Moran index I_i, calculated as follows:

$$I_i = \frac{n(x_i - \overline{X})}{\sum_{i=1}^{n}(x_i - \overline{X})^2}\sum_{j=1}^{n} W_{ij}(x_j - \overline{X}) \tag{25}$$

3) Dagum Gini Coefficient

To examine the spatial disparities in the three-system coupling coordination degree, the 31 provinces are grouped into eastern, central, western and north-eastern regions on the standard geographical classification.

We apply the Dagum Gini coefficient [25] to quantify regional differences in coupling coordination, with the overall coefficient defined below:

$$G = \frac{1}{2n^2\overline{y}}\sum_{a=1}^{k}\sum_{b=1}^{k}\sum_{i=1}^{n_a}\sum_{j=1}^{n_b} |y_{ai} - y_{bj}| \tag{26}$$

where n is the number of study subjects and $\overline{y}$ is the mean value of all study subjects, k denotes the number of subgroups, a and b represent different subgroups, respectively, and n_a and n_b represent the number of subjects in groups a and b, respectively. y_{ai} and y_{bj} represent the proportion of coupling coordination of any research object within groups a and b, respectively. The formulas for calculating intra- and inter-regional Gini coefficients are shown in equations (27) and (28), respectively:

$$G_{aa} = \frac{1}{2n_a^2\overline{y}_a}\sum_{i=1}^{n_a}\sum_{j=1}^{n_a} |y_{ai} - y_{aj}| \tag{27}$$

$$G_{ab} = \frac{1}{n_a n_b(\overline{y}_a + \overline{y}_b)}\sum_{i=1}^{n_a}\sum_{j=1}^{n_b} |y_{ai} - y_{bj}| \tag{28}$$

To further explore the sources of regional variation, this paper will decompose the Dagum Gini coefficient into within-group variation contribution (G_w), the contribution of between-group variation (G_{nb}) and hypervariance density (G_t). The calculation formula is shown below:

$$G_w = \sum_{a=1}^{k} G_{aa} p_a s_a \tag{29}$$

$$G_{nb} = \sum_{a=2}^{k}\sum_{b=1}^{a-1} G_{ab}(p_b s_a + p_a s_b) D_{ab} \tag{30}$$

$$G_t = \sum_{a=2}^{k}\sum_{b=1}^{a-1} G_{ab}(p_b s_a + p_a s_b)(1 - D_{ab}) \tag{31}$$

where $G_w + G_{nb} + G_t = G$. Here $p_a = n_a/n$ and $s_a = n_a\overline{y}_a/(n\overline{y})$ are the population and income shares of group a, and $D_{ab} = (h_{ab} - q_{ab})/(h_{ab} + q_{ab})$ is the relative affluence between groups a and b, with h_{ab} and q_{ab} defined as follows:

$$h_{ab} = \int_0^{\infty} dF_a(y)\int_0^{y}(y - x)dF_b(x) \tag{32}$$

$$q_{ab} = \int_0^{\infty} dF_b(y)\int_0^{y}(y - x)dF_a(x) \tag{33}$$

E. SPECIFICATION AND ROBUSTNESS

Three specification choices deserve comment. The spatial weight matrix is a first-order queen contiguity matrix, row-standardized; because Hainan shares no land border it is linked to Guangdong, the nearest province across the strait. The quantile regression follows the method-of-moments estimator of Machado and Santos Silva [26], which accommodates province fixed effects; the full coefficient table with province-clustered bootstrap standard errors from 800

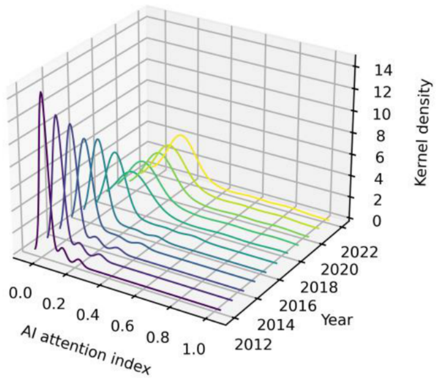

FIGURE 1. Characterization of the dynamic evolution of the AI Technology Attention level

replications is reported in Table IV rather than in graphical form alone. Finally, because D is bounded on the unit interval, the determinant regressions were re-estimated on its logit transform, which leaves the sign and significance of every coefficient unchanged.

V. RESULTS AND ANALYSIS

A. EVOLUTIONARY CHARACTERIZATION OF AI TECHNOLOGY ATTENTION

Figure 1 reports the kernel density of AI technology attention over the sample period. The national mean rises from 0.041 in 2012 to 0.189 in 2022, a more than fourfold increase, and the modal position moves steadily to the right. The distribution flattens and widens as it moves, so absolute dispersion across provinces grew even as every province advanced. The distribution is strongly right-skewed in every year, with a skewness coefficient between 2.9 and 3.4, indicating a small group of provinces whose search intensity far exceeds the rest. It remains single-peaked: the kernel estimate shows only a low right-tail shoulder, never a second mode of comparable height, so no polarization emerges.

B. EVOLUTIONARY CHARACTERIZATION OF THE ELECTROMAGNETIC INFRASTRUCTURE LAYER

Figure 2 reports the kernel density of the electromagnetic infrastructure index and the separate trajectories of its two layers. The composite index rises from 0.116 to 0.197 over the period, a far slower advance than that of demand. The decomposition by layer is the substantive result: the guided-wave sub-index rises from 0.164 to 0.297 while the free-space sub-index rises only from 0.098 to 0.160, so the transport tier pulled away from the access tier over the decade rather than advancing with it. The dispersion ordering predicted in Section II also holds, and holds by a wide margin. Take the ratio of the highest to the lowest provincial value in 2022. Mobile telephone penetration, a usage measure, differs by a factor of 2.0. Optical cable route density differs by a factor of 25.5. Switching capacity

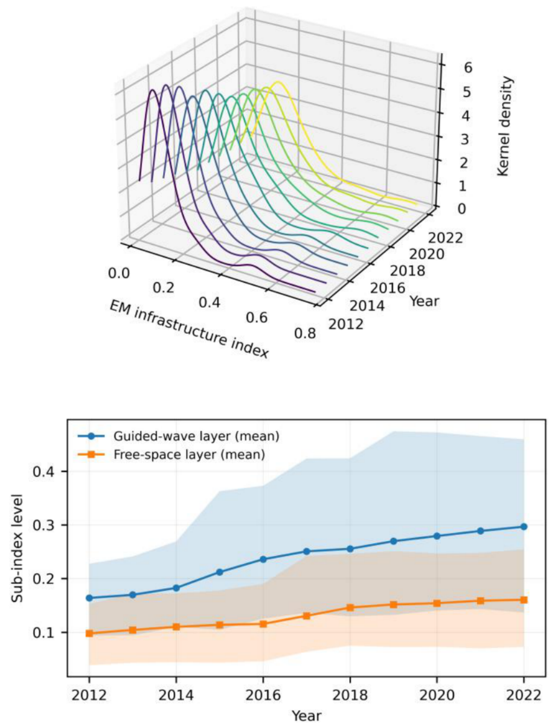

FIGURE 2. Dynamic evolution of the electromagnetic infrastructure index and of its guided-wave and free-space sub-indices

density, the areal measure of the access tier, differs by a factor of 878. Shanghai carries 11,268 units of switching capacity per ten-thousand square kilometers against 12.8 in Qinghai. The usage margin has very nearly closed while the areal deployment margin spans three orders of magnitude, which is what propagation-limited coverage economics predicts and what an aggregate infrastructure index would conceal.

C. EVOLUTIONARY CHARACTERIZATION OF REGIONAL E-COMMERCE DEVELOPMENT

Figure 3 reports the kernel density of regional e-commerce development. The national mean rises from 0.188 to 0.277, with the modal position moving right and the distribution widening, so absolute dispersion again increased. The series is not monotonic, dipping in 2013, 2017 and 2022, which reflects year-to-year variation in the enterprise survey indicators underlying the index. The distribution is right-skewed in every year, though the degree varies considerably (skewness between 0.21 in 2016 and 1.78 in 2021), and it stays single-peaked apart from low right-tail shoulders. This index excludes the two digital-infrastructure indicators used in earlier specifications, which now belong to the electromagnetic infrastructure subsystem.

D. THREE-SYSTEM COUPLING COORDINATION ANALYSIS

Figure 4 reports the three-system coupling coordination degree by province. The national mean rises from 0.293

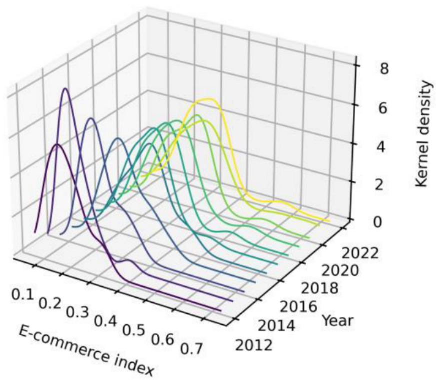

FIGURE 3. Dynamic evolution of the regional e-commerce development level

in 2012 to 0.448 in 2022, moving the country from level 3 to level 5 of the classification in Table II, and the provincial range in 2022 runs from 0.332 to 0.779. The eastern lead persists once physical capacity enters as a co-equal subsystem: Beijing and Shanghai lead by a wide margin at 0.779 and 0.723, followed by Tianjin, Zhejiang, Guangdong and Jiangsu clustered near 0.51, while Tibet, Xinjiang, Jilin, Gansu and Heilongjiang occupy the bottom between 0.332 and 0.382. The interpretation advanced here is cumulative: a stronger economic base supports denser deployment, which lowers the cost of the AI-mediated services that raise commercial activity, which funds further deployment. What the three-system measure adds is the ability to say which link in that chain is slack in any given province, and Section V.E does so.

Figure 5 reports the kernel density of the coupling coordination degree. The modal position moves steadily to the right, consistent with the rise in the national mean, while the distribution widens, so absolute dispersion increased. The distribution stays single-peaked, again with only a low right-tail shoulder rather than a second mode, and its right skew is pronounced and strengthens over the period, the skewness coefficient rising from 1.46 in 2012 to 2.21 in 2022: coordination improves across the board while a few provinces pull steadily further ahead. Two points should be kept distinct when reading this against Section V.H. A widening kernel density and a falling Gini coefficient are not in conflict: the former measures absolute spread, the latter inequality relative to the mean. Both are observed here, and the reading is that every province improved while the leaders improved faster in absolute terms.

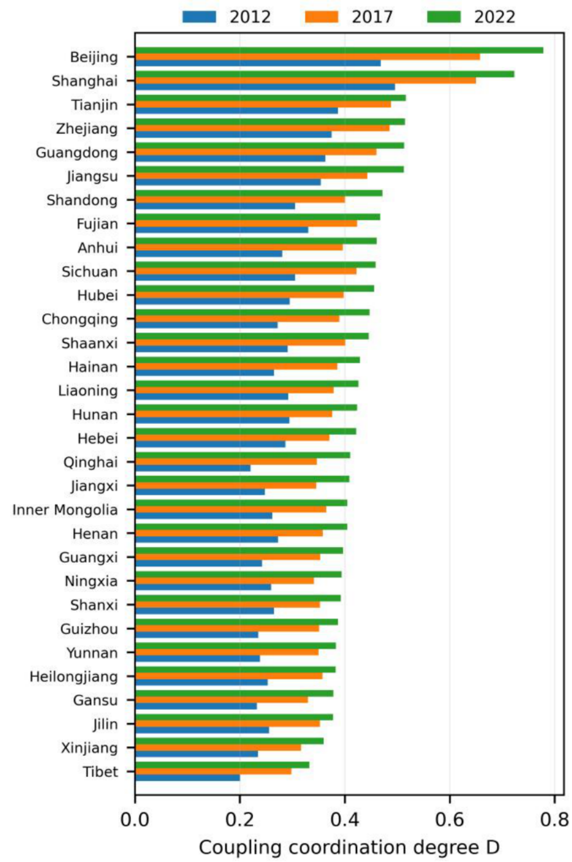

FIGURE 4. Three-system coupling coordination evaluation

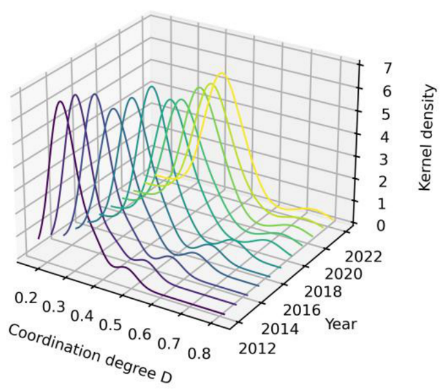

FIGURE 5. Dynamic evolution of the three-system coupling coordination degree

E. WHERE IS THE ELECTROMAGNETIC LAYER THE BINDING CONSTRAINT

Applying the diagnostic of Section IV to each of the 341 province-year observations yields the identity of the binding subsystem, the severity measure lambda, and, for electromagnetically constrained observations, the layer attribution delta. Table III reports the composition by year and Figure 6 maps it by province for 2012 and 2022.

The headline result is that the binding subsystem migrates. In 2012 demand was the limiting factor in 30 of 31 provinces and the electromagnetic layer in none: attention to AI was so low relative to installed capacity and commercial activity that nothing else could bind. By 2017 the electromagnetic layer had become binding in 7 provinces, and by 2022 in 14 of 31, against 15 still limited by demand and 2 by e-commerce development. Over the full panel, 77 of 341 observations, or 22.6%, are electromagnetically constrained. This is the paper's central empirical claim: as public attention to AI rose, the constraint on coordinated development shifted from what regions wanted to what their networks could carry.

The composition of that constraint is equally clear. Of the 77 electromagnetically constrained observations, 63 (81.8%) are access-limited and 14 (18.2%) fiber-limited, and the two groups differ exactly as Hypothesis H2 predicts. Access-limited province-years have a median land area of 18.59 ten-thousand square kilometers against 1.64 for fiber-limited ones (Welch $t = 6.63$, $p = 9.2\text{e-}09$) and a median population density of 190 against 1,333 persons per square kilometer ($t = -5.34$, $p = 1.1\text{e-}04$). Ranked by frequency, the access-limited group is led by Chongqing (7 province-years), Shaanxi, Qinghai, Ningxia and Jilin (6 each), Liaoning and Fujian (5), Gansu (4), and Inner Mongolia, Jiangxi and Heilongjiang (3 each), with Tibet, Hubei and Hainan appearing twice and Xinjiang, Tianjin and Shanxi once. The group is therefore mostly, though not exclusively, western and north-eastern: Fujian and Jiangxi are neither large nor thinly settled, and their appearance indicates that rapid demand growth can outrun access capacity even in compact provinces. The fiber-limited group contains only Beijing (9 province-years) and Hainan (5), the two units that combine dense settlement with structurally limited transit routing, a municipality and an island. H2 is supported.

Hypothesis H3 is not supported, and the reason is instructive. The absolute gap between AI technology attention and realized e-commerce development is smaller, not larger, among electromagnetically constrained observations (0.129 against 0.173, Welch $t = -4.01$, $p = 1.1\text{e-}04$). Part of this is mechanical: when U2 is the minimum of the three subsystems, U1 and U3 are by construction the two upper values and therefore tend to lie closer together than when one of them is itself the minimum. The underlying intuition of H3 does survive in a form the diagnostic can test directly: the attention-development gap widens with the severity of imbalance, regressing on lambda with a slope of 0.210 (standard error 0.019, $r = 0.523$, $p = 2.8\text{e-}25$). We report H3 as rejected as stated and treat the lambda relationship as an exploratory finding rather than a confirmed prediction.

TABLE 3. Binding Subsystem by Year: Counts and Shares

Year	Demand (U1)	EM layer (U2)	E-commerce (U3)	Access-ltd	Fiber-ltd
2012	30 (96.8%)	0 (0.0%)	1 (3.2%)	0	0
2013	30 (96.8%)	0 (0.0%)	1 (3.2%)	0	0
2014	30 (96.8%)	1 (3.2%)	0 (0.0%)	0	1
2015	30 (96.8%)	1 (3.2%)	0 (0.0%)	0	1
2016	27 (87.1%)	4 (12.9%)	0 (0.0%)	2	2
2017	22 (71.0%)	7 (22.6%)	2 (6.5%)	5	2
2018	17 (54.8%)	12 (38.7%)	2 (6.5%)	10	2
2019	20 (64.5%)	9 (29.0%)	2 (6.5%)	7	2
2020	13 (41.9%)	16 (51.6%)	2 (6.5%)	14	2
2021	16 (51.6%)	13 (41.9%)	2 (6.5%)	12	1
2022	15 (48.4%)	14 (45.2%)	2 (6.5%)	13	1

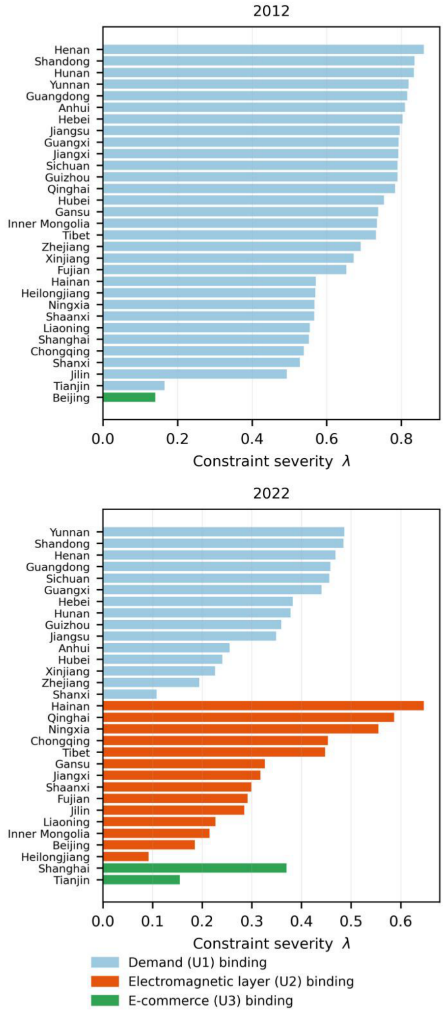

FIGURE 6. Binding-constraint category by province, 2012 and 2022

F. DETERMINANTS OF THE THREE-SYSTEM COUPLING COORDINATION DEGREE

This subsection investigates the determinants of the three-system coupling coordination degree. The independent variables are regional economic development (AGDP, per capita GDP in logs), financial support (GS, fiscal expenditure over GDP), R&D intensity (RD, internal R&D expenditure over GDP), industrial structure (IS, the ratio of tertiary to secondary output), urbanization (UR) and human capital (HC, the higher-education enrolment rate). Estimation follows the method-of-moments quantile regression of Machado and Santos Silva [26] with province fixed effects; Figure 7 plots

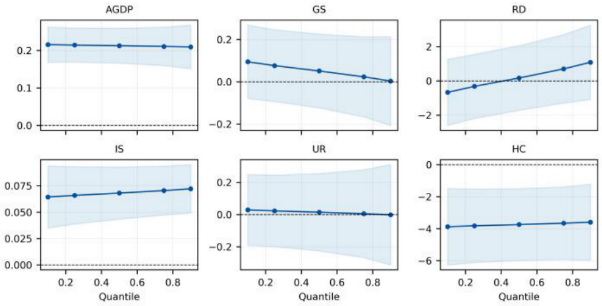

FIGURE 7. Determinants of the coupling coordination degree by quantile

TABLE 4. Method-of-Moments Quantile Regression: Coefficients and Standard Errors. Province-Clustered Bootstrap Standard Errors from 800 Replications in Parentheses; *** $p < 0.01$, ** $p < 0.05$, * $p < 0.10$

Variable	Q10	Q25	Q50	Q75	Q90
	0.215***	0.214***	0.212***	0.211***	0.209***
AGDP	(0.024)	(0.023)	(0.024)	(0.026)	(0.030)
	0.095	0.076	0.051	0.023	0.003
GS	(0.088)	(0.087)	(0.089)	(0.097)	(0.107)
	-0.667	-0.317	0.171	0.704	1.089
RD	(0.985)	(0.954)	(0.962)	(1.018)	(1.106)
	0.064***	0.066***	0.068***	0.070***	0.072***
IS	(0.015)	(0.014)	(0.013)	(0.012)	(0.012)
	0.029	0.023	0.015	0.005	-0.001
UR	(0.112)	(0.113)	(0.122)	(0.139)	(0.159)
	-3.882***	-3.826***	-3.748***	-3.662***	-3.600***
HC	(1.219)	(1.172)	(1.145)	(1.158)	(1.212)

the coefficients across quantiles and Table IV reports them with province-clustered bootstrap standard errors. Regional economic development is positive and significant at the 1% level at every quantile, with a coefficient close to 0.212 throughout, and industrial structure is likewise positive and significant, rising gently from 0.064 at the tenth percentile to 0.072 at the ninetieth. Human capital enters negatively and significantly (about -3.75); this is a conditional association rather than a causal effect, and it most plausibly reflects that provinces with large student populations relative to their own size include several northern and north-eastern units whose networks are comparatively thin. Financial support, R&D intensity and urbanization are not statistically significant at any quantile. The scale coefficients are small for all variables except R&D intensity, so the marginal effects are close to constant across the distribution: the determinants of coordination operate similarly on well-coordinated and poorly coordinated provinces alike.

G. SPATIAL DEPENDENCE OF THE THREE-SYSTEM COUPLING COORDINATION

Table V reports the global spatial dependence of the three-system coupling coordination degree. Moran's I is positive and significant at the 1% level in every year of the sample, so coordination is spatially clustered rather than randomly distributed across provinces, and Hypothesis H1 is supported. The statistic declines from 0.418 in 2012 to 0.296 in 2022, indicating that the spatial structure, while still strong, loosened somewhat as construction spread inland.

TABLE 5. Global Moran Index

Year	Moran's I	Z	P-value
2012	0.4184***	3.9688	0.0001
2013	0.4356***	4.1330	0.0000
2014	0.4255***	4.1037	0.0000
2015	0.3857***	3.7527	0.0002
2016	0.3271***	3.2383	0.0012
2017	0.3301***	3.3319	0.0009
2018	0.2976***	3.0816	0.0021
2019	0.3178***	3.2625	0.0011
2020	0.3134***	3.2526	0.0011
2021	0.2755***	2.8630	0.0042
2022	0.2962***	3.1027	0.0019

Note: ***, **, and * represent significant at the 1%, 5%, and 10% statistical levels, respectively.

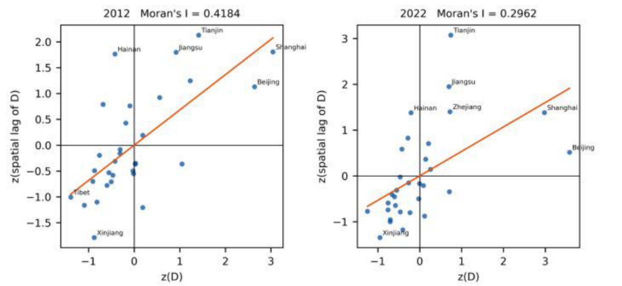

FIGURE 8. Moran scatter plot

Figure 8 shows the Moran scatter plots for 2012 and 2022. Most provinces fall in the first and third quadrants, 23 of 31 in 2012 and 25 of 31 in 2022, so the dominant local pattern is high-high and low-low clustering and it strengthened over the period. The high-high cluster is the eastern seaboard, comprising Beijing, Tianjin, Shanghai, Jiangsu, Zhejiang, Shandong and Fujian, joined by Anhui in 2022. The low-low cluster comprises the western and north-eastern provinces together with much of the center. The few high-low units, Sichuan, Hubei and Guangdong, are inland or southern growth poles that outperform their immediate neighbors, and Jiangxi, Hebei and Hainan occupy the low-high quadrant, lying adjacent to stronger provinces without yet matching them.

H. REGIONAL DIFFERENCES IN THE THREE-SYSTEM COUPLING COORDINATION

The overall regional differences are analyzed in Figure 9. The Dagum Gini coefficient of the three-system coupling coordination degree falls from 0.1168 in 2012 to 0.0964 in 2022, a decline of about 17%, with local peaks in 2015 and 2019. Relative inequality in coordination therefore narrowed over the period, even as the kernel density estimates of Section V.D show absolute dispersion widening; as noted there, the two statements are compatible and jointly describe a distribution whose mean and spread both rose while the spread grew more slowly than the mean.

Analysis of intra-regional differences is reported in Figure 10. The eastern region displays by far the highest internal inequality throughout, moving between 0.105 and 0.118

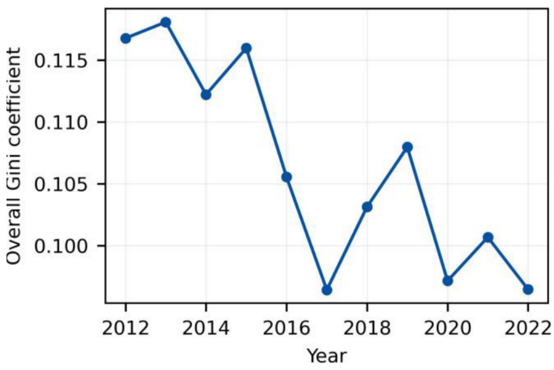

FIGURE 9. Overall regional differences

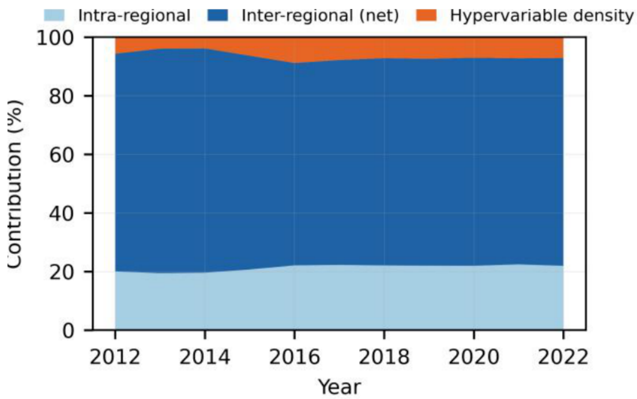

FIGURE 11. Sources and contributions of regional differences

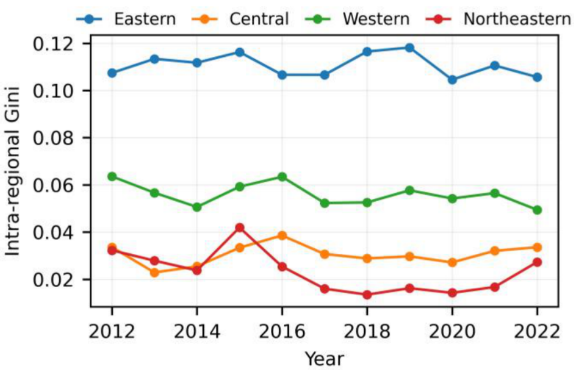

FIGURE 10. Intra-regional differences

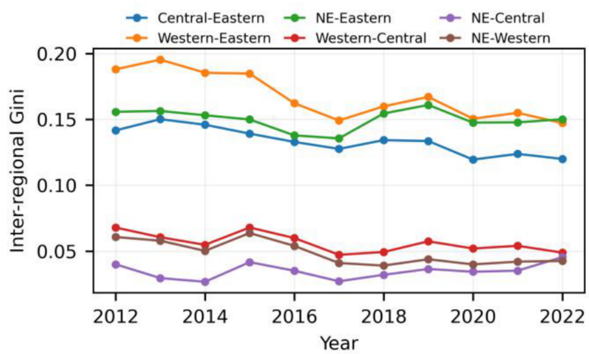

FIGURE 12. Inter-regional differences

and ending at 0.106, essentially where it began; the region contains both the national leaders and several much weaker provinces. The western region declines from 0.064 to 0.049, the clearest internal convergence in the sample. The central region is the most stable, fluctuating between 0.023 and 0.039 around a mean of 0.031 with no trend, and the north-east falls from 0.032 to 0.014 by 2018 before rising again to 0.027 by 2022.

Figure 11 presents the sources of the total difference, decomposing it into intra-regional, net inter-regional and hypervariable density components. Inter-regional differences dominate throughout, contributing 74.3% of the total in 2012 and 71.0% in 2022. The intra-regional contribution rises modestly from 20.1% to 22.0%, and the hypervariable density term, which captures overlap between regional distributions, moves from 5.6% to 7.1%. The policy reading is unchanged from the two-system literature: the gap between regions, not within them, is what drives national dispersion in coordination.

Inter-regional differences are analyzed in Figure 12. Five of the six pairwise coefficients decline over the period; the north-eastern-central pair is the exception, edging up from 0.040 to 0.045. The eastern-western pair is the largest throughout, falling from 0.188 to 0.147; the eastern-north-eastern pair falls from 0.156 to 0.150 and the eastern-central pair from 0.142 to 0.120. The three pairs not involving the east are much smaller, between 0.027 and 0.068 across the sample. The east against everywhere else remains the principal axis of difference.

VI. DISCUSSION

A. INTERPRETATION AND RELATION TO PRIOR WORK

The framework developed here departs from the regional digital-economy literature in treating the physical layer as an object of measurement rather than as a background condition, and it departs from the communications engineering literature in asking where, in an administrative geography, the capability that literature creates has actually been installed. The two bodies of work make contact at a single point: the cost of delivering a given service level over a given area is set by propagation, and propagation varies with geography in ways that economic aggregates do not capture. The estimates bear this out in a specific and, to us, unexpected way. The conventional reading of China's digital-economy geography is that the east leads because demand and commercial capability are concentrated there, and our coordination ranking reproduces that ordering. But the binding-constraint decomposition shows that the ordering is now produced by a different mechanism than it was a decade ago. In 2012 demand was the limiting subsystem almost everywhere, so the east led because it wanted AI first. By 2022 attention had risen nationally to the point where, in 14 of 31 provinces, the electromagnetic layer had become the shortest board. The east now leads because it can carry what it wants, not merely because it wants more. Prior work that nests infrastructure inside a composite outcome index cannot see this transition, because the quantity that changed is the identity of the minimum rather than the level of the aggregate.

One result that the design anticipates deserves emphasis whichever way it comes out. If the coordination degree is found to rise while the absolute dispersion of its distribution also widens, the two statements are not in conflict: the kernel density estimate describes the absolute spread of provincial levels, whereas the Gini decomposition describes inequality relative to the mean. A period in which all provinces improve but the leaders improve faster in absolute terms will show exactly this combination. Earlier treatments of this material reported both patterns without reconciling them; the distinction between absolute dispersion and relative inequality should be stated explicitly wherever both measures are discussed.

B. IMPLICATIONS FOR INFRASTRUCTURE DEPLOYMENT

The practical value of the binding-constraint diagnostic is that it converts a coordination index into a deployment instruction. Three implications follow, each tied to a specific result rather than offered as general advice.

First, for province-years classified as access-limited, the marginal return lies in radio site density rather than in transport capacity, and the relevant engineering levers are those that reduce the cost of areal coverage: higher-gain and wideband radiators, MIMO arrays that raise per-site capacity, and band selection that trades bandwidth for reach. The device-level advances reported in this journal [8], [9], [10], [11] act directly on this margin, and the diagnostic identifies the regions where their deployment value is highest.

Second, for province-years classified as fiber-limited, additional radio sites will not relieve the constraint, because the bottleneck lies in backhaul and transport rather than in the air interface; here the relevant margin is route extension and fiber-to-the-premises conversion. Distinguishing these two cases is the main operational contribution of the paper, and it is not available from any aggregate digital-infrastructure index.

Third, where the binding subsystem is demand rather than infrastructure, further physical construction yields little near-term coordination gain, and the constraint is better addressed through the adoption-side channels identified in the e-commerce literature. On the 2022 estimates the three cases divide as follows. Fourteen provinces are electromagnetically constrained: Hainan, Qinghai, Ningxia, Chongqing, Tibet, Gansu, Jiangxi, Shaanxi, Fujian, Jilin, Liaoning, Inner Mongolia, Beijing and Heilongjiang. Thirteen of the fourteen are access-limited, so for those the marginal return lies in radio-access density rather than in transport. Beijing alone is fiber-limited in that year, and there additional radio capacity would not relieve the constraint. Hainan is the one province that switches between the two categories over the sample, appearing as fiber-limited in five years and access-limited in two, which is consistent with an island whose transport dependence on a single submarine crossing eases as that crossing is upgraded. Fifteen provinces, including Yunnan, Shandong, Henan, Guangdong, Sichuan and Guangxi, remain demand-limited, so physical construction there yields little near-term coordination gain and the adoption-side channels are the operative margin. Shanghai and Tianjin are limited by e-commerce development itself, having built ahead of what their commercial base currently uses.

C. LIMITATIONS AND FUTURE RESEARCH

Five limitations qualify these results. First, the Baidu Index measures attention, not technical capability or deployment; a province may search intensively for AI terms without hosting any AI production capacity, and the normalization by internet users mitigates but does not remove this gap between interest and competence. Second, and specific to this study, the free-space layer is measured by mobile switching capacity rather than by a count of radio sites, because provincial site counts are not published for the sample period. Switching capacity measures installed network capacity and, divided by land area, how densely that capacity is distributed; it is not a direct measure of radio coverage and cannot distinguish many low-capacity sites from few high-capacity ones. The layer attribution in Section V.E should therefore be read as separating transport-constrained from access-constrained provinces rather than as a statement about site counts, and confirming it against operator site registries or provincial 5G deployment series is the most valuable robustness check that remains open. Third, provincial aggregation conceals intra-provincial variation that is likely to be large precisely on the dimension of interest, since coverage and fiber density differ far more between a provincial capital and its rural periphery than between two provincial means; prefecture-level or grid-level analysis would be a natural extension. Fourth, the analysis is descriptive and distributional rather than causal. The quantile regressions identify conditional associations, and no claim of identification is made; quasi-experimental designs built on staged infrastructure programs would be required to establish causal effects, and are a clear direction for future work. Fifth, the sample ends in 2022 and therefore predates both the large-scale commercial deployment of generative AI in Chinese e-commerce and the densest phase of 5G construction. Extending the panel through 2024 would allow the free-space layer to be measured directly by 5G site density over a meaningful span, and would test whether the generative-AI period raised the electromagnetic threshold in the way Section II anticipates.

VII. CONCLUSION

This paper has argued that the physical substrate of regional digital-economy development is electromagnetic, that it consists of two layers whose deployment economics differ because their propagation physics differs, and that regional analysis which aggregates them forfeits the ability to say which layer constrains growth. Acting on that argument, we did three things. We constructed a provincial indicator system for China's electromagnetic communication infrastructure that separates guided-wave transport from free-space access and expresses each in areal-density as well as absolute terms. We generalized the coupling coordination model to three subsystems, of which the conventional two-system form is a special case. And we introduced a binding-constraint diagnostic that identifies, for each province and year, whether the electromagnetic layer is the limiting subsystem and, if so, which layer is responsible.

The estimates show a national coupling coordination degree rising from 0.293 in 2012 to 0.448 in 2022, that is from level 3 to level 5 of the classification adopted here, with the provincial range in the final year running from 0.332 to 0.779. The spatial structure is significant and positive in every year, with Moran's I falling from 0.418 to 0.296 as construction spread inland, and high-high and low-low clustering dominant throughout. Relative dispersion narrows, the Dagum Gini falling from 0.117 to 0.096, while inter-regional differences supply between 69% and 77% of what dispersion remains. The binding-constraint results are the substantive contribution. The limiting subsystem migrates from demand to physical capacity over the decade: the electromagnetic layer binds in no province in 2012 and in fourteen by 2022. Among the 77 electromagnetically constrained province-years, 81.8% are limited by the free-space access layer and 18.2% by guided-wave transport. The access-limited group is systematically larger in area and thinner in settlement, exactly as propagation-limited coverage economics predicts.

The significance of these findings is that they render a socio-economic coordination measure legible as a deployment-priority map. For a communications engineering readership, the diagnostic indicates where advances in radio-access technology are most likely to relieve an actual constraint, and where they will not, because the limitation lies in guided-wave transport or in demand. The boundary conditions should be kept in view: the results describe provincial averages within a single national administrative and spectrum regime over 2012–2022, and their transfer to other regulatory settings or finer spatial scales should not be assumed.

AVAILABILITY OF DATA AND MATERIALS

The datasets used and/or analyzed during the current study were available from the corresponding author on reasonable request.

AUTHOR CONTRIBUTIONS

First Author: Data analysis and Writing. Second Author: Methodology and Formal Analysis. Third and Fourth Author: Resources and Validation

CONFLICT OF INTEREST

The authors declare no conflict of interest.

FUNDING

Shandong Provincial Natural Science Foundation Program: ZR2022MF334

Shandong Provincial Institute of Innovation and Development Research 2024 Support Project for Scientific and Technological Innovation and Development: SHZB2024-828

Jinan City-University Integration Development Strategic Engineering Project: JNSX2025023

ACKNOWLEDGMENT

Not applicable.

REFERENCES

[1] R. J. Essiambre and R. W. Tkach, "Capacity trends and limits of optical communication networks," Proceedings of the IEEE, vol. 100, no. 5, pp. 1035-1055, 2012, doi: 10.1109/JPROC.2012.2182970.

[2] P. J. Winzer, D. T. Neilson, and A. R. Chraplyvy, "Fiber-optic transmission and networking: the previous 20 and the next 20 years," Optics Express, vol. 26, no. 18, pp. 24190-24239, 2018, doi: 10.1364/OE.26.024190.

[3] T. S. Rappaport, Wireless Communications: Principles and Practice, 2nd ed. Upper Saddle River, NJ: Prentice Hall, 2002, ISBN 0-13-042232-0.

[4] J. G. Andrews, S. Buzzi, W. Choi, et al., "What will 5G be?" IEEE Journal on Selected Areas in Communications, vol. 32, no. 6, pp. 1065-1082, 2014, doi: 10.1109/JSAC.2014.2328098.

[5] G. P. Agrawal, Fiber-Optic Communication Systems, 4th ed. Hoboken, NJ: Wiley, 2010, doi: 10.1002/9780470918524.

[6] D. J. Richardson, J. M. Fini, and L. E. Nelson, "Space-division multiplexing in optical fibres," Nature Photonics, vol. 7, no. 5, pp. 354-362, 2013, doi: 10.1038/nphoton.2013.94.

[7] T. S. Rappaport, S. Sun, R. Mayzus, et al., "Millimeter wave mobile communications for 5G cellular: it will work!" IEEE Access, vol. 1, pp. 335-349, 2013, doi: 10.1109/ACCESS.2013.2260813.

[8] A. D. Tadesse, O. P. Acharya, and S. Sahu, "A compact planar four-port MIMO antenna for 28/38 GHz millimeter-wave 5G applications," Advanced Electromagnetics, vol. 11, no. 3, pp. 16-25, 2022, doi: 10.7716/aem.v11i3.1947.

[9] P. K. Patnaik, M. Murali, H. C. Mohanta, and D. C. Panda, "Miniaturized fractal antenna design for 6-GHz 5G advanced communications," Advanced Electromagnetics, vol. 14, no. 3, pp. 1-8, 2025, doi: 10.7716/aem.v14i3.2482.

[10] L. Guo, "A super-wideband miniaturized graphene-based folded monopole antenna," Advanced Electromagnetics, vol. 14, no. 1, pp. 1-7, 2025, doi: 10.7716/aem.v14i1.2546.

[11] X. H. Yang, Y. Z. Ma, Z. Chen, et al., "A planar high-gain circularly polarized dipole antenna based on PRAMC for 2.45 GHz ISM band," Advanced Electromagnetics, vol. 15, no. 2, pp. 11-20, 2026, doi: 10.7716/aem.v15i2.2926.

[12] Y. Mao, C. You, J. Zhang, et al., "A survey on mobile edge computing: the communication perspective," IEEE Communications Surveys and Tutorials, vol. 19, no. 4, pp. 2322-2358, 2017, doi: 10.1109/COMST.2017.2745201.

[13] W. Saad, M. Bennis, and M. Chen, "A vision of 6G wireless systems: applications, trends, technologies, and open research problems," IEEE Network, vol. 34, no. 3, pp. 134-142, 2020, doi: 10.1109/MNET.001.1900287.

[14] T. Davenport, A. Guha, D. Grewal, et al., "How artificial intelligence will change the future of marketing," Journal of the Academy of Marketing Science, vol. 48, no. 1, pp. 24-42, 2020, doi: 10.1007/s11747-019-00696-0.

[15] E. Gomez-Herrera, B. Martens, and G. Turlea, “The drivers and impediments for cross-border e-commerce in the EU,” Information Economics and Policy, vol. 28, pp. 83-96, 2014, doi: 10.1016/j.infoecopol.2014.05.002.
[16] Y. Kim and R. A. Peterson, “A meta-analysis of online trust relationships in e-commerce,” Journal of Interactive Marketing, vol. 38, no. 1, pp. 44-54, 2017, doi: 10.1016/j.intmar.2017.01.001.
[17] S. Ma, Y. Chai, and H. Zhang, “Rise of cross-border e-commerce exports in China,” China and World Economy, vol. 26, no. 3, pp. 63-87, 2018, doi: 10.1111/cwe.12243.
[18] V. Hovelaque, L. Soler, and S. Hafsa, “Supply chain organization and e-commerce: a model to analyze store-picking, warehouse-picking and drop-shipping,” 4OR, vol. 5, no. 2, pp. 143-155, 2007, doi: 10.1007/s10288-006-0013-5.
[19] A. Andonov, G. Dimitrov, and V. Totev, “Impact of e-commerce on business performance,” TEM Journal, vol. 10, no. 4, pp. 1558-1564, 2021, doi: 10.18421/TEM104-09.
[20] C. L. Hwang and K. Yoon, Multiple Attribute Decision Making: Methods and Applications. Berlin: Springer, 1981, doi: 10.1007/978-3-642-48318-9.
[21] C. E. Shannon, “A mathematical theory of communication,” Bell System Technical Journal, vol. 27, no. 3, pp. 379-423, 1948, doi: 10.1002/j.1538-7305.1948.tb01338.x.
[22] B. W. Silverman, Density Estimation for Statistics and Data Analysis. London: Chapman and Hall, 1986, ISBN 0-412-24620-1.
[23] P. A. P. Moran, “Notes on continuous stochastic phenomena,” Biometrika, vol. 37, nos. 1-2, pp. 17-23, 1950, doi: 10.1093/biomet/37.1-2.17.
[24] L. Anselin, “Local indicators of spatial association - LISA,” Geographical Analysis, vol. 27, no. 2, pp. 93-115, 1995, doi: 10.1111/j.1538-4632.1995.tb00338.x.
[25] C. Dagum, “A new approach to the decomposition of the Gini income inequality ratio,” Empirical Economics, vol. 22, no. 4, pp. 515-531, 1997, doi: 10.1007/BF01205777.
[26] J. A. F. Machado and J. M. C. Santos Silva, “Quantiles via moments,” Journal of Econometrics, vol. 213, no. 1, pp. 145-173, 2019, doi: 10.1016/j.jeconom.2019.04.009.